

## HIGH RESOLUTION HEAT FLOW DSC: APPLICATION TO STUDY OF PHASE TRANSITIONS, AND PORE SIZE DISTRIBUTION IN SATURATED POROUS MATERIALS

L. G. HOMSHAW

*Station de Science du Sol – I.N.R.A. Route de St. Cyr, 78000 Versailles – France*

(Received April 3, 1979; in revised form December 5, 1980)

Suitable container design permits very high temperature and differential temperature resolution in DSC even when relatively large ( $\approx 0.14 \text{ cm}^3$ ) samples are used; and thus energy signals associated with phase change occurring over large temperature intervals may be analysed in differential elements.

An original and powerful high resolution low temperature DSC technique (the authors  $\psi$  plot") for studying and comparing pore size distributions (PSD) in water saturated samples (for pores having Kelvin radii between 1,2 and about 500 nm) is given, together with an application which shows that the PSD in a water saturated organic ion exchanger could be obtained from analysis of three Gaussian distributions which precisely generate a curve which is an excellent empirical fit to the recorded low temperature exotherm obtained by freezing pure water within the sample.

The temperature at which liquids and solids change phase in porous materials depends upon pore size [1]. For water the lowering of freezing or melting temperatures is inversely proportional to the pore Kelvin radius [2]. For cylindrical pores the Kelvin radius is equivalent to the radius of the cylinder, whereas for parallel-sided fissures it corresponds to the wall to wall distance [3].

Low temperature high resolution DSC is a powerful tool for investigating water and solution behaviour in porous materials [2] and knowledge of the relationship between phase transition temperature and pore size allows the distribution of pore sizes in wet porous materials to be determined. The shape of a pore determines the extent to which hysteresis occurs between the equilibrium freezing and melting temperatures of water (or salt eutectic) in the pore space [2]. For materials which swell in contact with water or for materials which contain "ink-bottle" shaped pores, monitoring of the freezing and melting behaviour of pure water in the substance gives quick and valuable information about the geometry of the pore spaces—these applications being suitable for studying pore sizes up to about 500 nm Kelvin radius, which size corresponds, for ice, to a lowering melting temperature of about  $0.1^\circ$  [2]. In this report a description is given of how DSC investigations may be optimized for this type of study by appropriate choice of experimental conditions, some modifications to standard equipment and suitable sample container design.

Exotherms or endotherms corresponding to water changing phase (under equilibrium conditions) within porous materials, are curves which occur over a temper-

ature range the magnitude of which depends upon the distribution of pore sizes within the substances. A pore size class having a mean kelvin radius,  $\bar{r} \pm \Delta r$  includes all the pores in the material having a kelvin radius  $r$  such that  $(\bar{r} + \Delta r) > r > (\bar{r} - \Delta r)$ . Therefore, because the Kelvin radius,  $r$ , determines the equilibrium freezing temperature of the pore water, it is essential for application of this DSC technique to know precisely in which temperature interval the water contained in pores of a given class freezes. Thus, not only is it necessary to have a system which permits accurate analytical study (or "deconvolution") of the DSC curves but it is also necessary to have high resolution measurement of the samples temperature and to be sure that temperature gradients within the sample are of negligible importance.

If it were possible to obtain a water saturated porous sample in which all the pores were cylindrical and of identical size, then at the equilibrium freezing temperature of the water in the pores, all the freezable water in the sample would freeze (being nucleated by the bulk ice in the system). The energy signal associated with this type of reaction is of very short duration and the DSC exotherm registered has been described as a "ballistic" curve resulting from a "ballistic shock" of very short duration [4]. This type of curve will be discussed in some detail below. In practice the DSC curve resulting from the energy associated with the equilibrium freezing of water in a porous material as a function of temperature may be considered as being an envelope corresponding to the summation in time of a very large number of discrete energy signals each one modulated in its intensity by the number of pores in a given class and by the apparent variation of latent heat with freezing temperature. Each one of these "quasi instantaneous" signals would give rise to a ballistic DSC curve [5]. It is therefore, interesting to study the factors (arising from instrumentation and experimental procedure) which could influence the form of a simple DSC ballistic curve. This study is of general use in microcalorimetry as it also provides a rapid method whereby the resolution of a DSC system may be investigated.

#### *Ballistic calorimetric curves*

Thermal phenomena of short duration (associated, for example, with quasi-instantaneous ionic reactions, heats of mixing and immersion [6]) give rise to ballistic calorimetric curves. The form of curves of this type may be predicted from analyses of heat transfer within the sample, between the sample and its container and between the container and the calorimeter. It has been shown [7] that the mathematical function which predicts the shape of ballistic calorimetric curves is a sum of many exponential terms in which the time constants very rapidly diminish in size so that, in practice the first two terms often give a very good fit to a DSC ballistic curve registered [4, 8]. In our experience, tests conducted using a number of different size samples and a variety of container designs often result in ballistic DSC curves which may be very satisfactorily fitted to by the simple expression:

$$H = K[\exp(-\beta t) - \exp(-\beta^* t)] \quad (1)$$

which is an expression identical in form to that given by Calvet and Prat [4] in an analytical study of calorimetric curves resulting from energy signals of very short duration (relative to the time constant of the apparatus), and where here,  $H$  represents the height of the DSC curve above the baseline at a time  $t$  measured from a time origin coincident with the start of the quasi-instantaneous energy signal. The base-line is the line  $H = 0$  and corresponds to the quasi-steady state condition that is, when  $dQ/dt = 0$  where  $Q$  is the amount of heat involved in the reaction and where under suitable circumstances,  $dQ/dt$  is directly proportional to  $H$  [4]. The positive constant  $K$  in equation (1) is accurately known and depends upon sample mass and the recorder sensitivity, and  $\beta$  and  $\beta^*$  ( $\beta^* > \beta$ ) are positive numbers. The expression "apparent proportional heat transfer coefficient" [5] has been used to describe  $\beta$  (the word proportional refers to the series of thermocouples constituting the fluxmeter). The time constant of a heat flow DSC is defined [4] by  $1/\beta$  and may be evaluated from the exponential relaxation curve after the finish of a reaction.

In order to further discuss the physical significance of the exponential terms in equation (1) in relation to heat flow and signal resolution in a low temperature heat flow microcalorimeter we consider a DSC system in which the sample and reference wells are connected by a series of thermocouples (the fluxmeter) the junctions of which are joined to all the external surfaces of the highly conducting metallic wells of the calorimeter via a thin layer of cement which also provides electrical insulation. The layer of cement and the finite resistance to heat flow afforded by the thermocouples of the fluxmeter constitute a thermal resistance which, as experience shows with our apparatus, is practically constant in the temperature interval  $+10^\circ \rightleftharpoons -60^\circ$ . The resistance to heat flow up and around the highly conducting cylindrical metallic wells of the calorimeter is negligible in relation to this latter thermal resistance. During scanning at a sufficiently slow rate we may assume that in the absence of sample container or sample, a quasi-instantaneous energy signal coming from any point on an inner surface of the well at the sample side of the fluxmeter results in a uniform increase of temperature on the inner surface of the well in a very short time. For reactions involving small energy exchange in which the reference temperature is insignificantly changed by the reaction, the time, in practice, necessary to completely register the resulting ballistic DSC curve will depend almost entirely upon the rate at which heat is conducted through the fluxmeter and its connections. After a quasi-instantaneous reaction, therefore, the relaxation curve of the DSC trace would reasonably be expected to be single exponential function in accordance with Newton's law of cooling. The first exponential term in Eq. (1) represents this relaxation curve. Use of this exponential relaxation curve has been described by Vold [9] to quantify DTA data without knowledge of the sample thermal conductivity, and this exponential term is analogous to the first term in an infinite series proposed in a detailed mathematical analysis of DTA data [10], (other solutions of the heat flow equation for regions of more complicated thermal geometry may be studied in [11]). The physical significance of the second exponential term in Eq. (1) is that it relates to the rate at which the temperature of the inner surface of the sample well rises.

*Effect of sample and sample container*

Ideal instantaneous energy signals are rarely generated in DSC work and it is necessary to consider the case where a sample of finite size having particular thermal characteristics is contained within a sample container having a particular thermal geometry. Experience shows that under these circumstances Eq. (1) is still a good fit to recorded ballistic curves and that the parameters  $\beta$  and  $\beta^*$  depend upon the thermal characteristics of the sample and sample container.

The fastest response time and best differential signal resolution are obtained from consideration of the return curve representing relaxation after an "instantaneous" energy signal has been given to one side of the fluxmeter assemblage — in the absence of sample or containers. It is desirable that the time response of the complete assemblage (sample, container and fluxmeter) closely approaches the fastest time response possible.

Let us suppose that the sample is held in a closed container and that a similar, but empty, container is used as the reference. The containers are brightly polished so as to reduce heat loss by radiation and the region above the containers and calorimeter wells is evacuated to avoid heat loss by convection. Under these conditions heat resulting from a quasi instantaneous energy signal from within the sample will not necessarily result in a quasi-instantaneous temperature rise on the inner surface of the sample well (a limiting case being the one in which the sample container is a closed Dewar vessel). This is due to the time necessary for the heat generated to dissipate itself through the sample, across the thermal resistance between the sample and the inside of the container, through the container walls and across the thermal resistance between the container and the fluxmeter well. Although, with suitable experimental design, a perfect thermal contact between the container and fluxmeter may be assumed to exist, the sample size and thermal characteristics, as well as the thermal geometry of the container, need to be taken into consideration when studying the resolution of such a DSC system. For a high resolution system it is desirable to distribute the sample in such a manner that heat is dissipated throughout the sample in a quasi-instantaneous fashion, or in other words, arrange the sample in such a way that its thermal diffusivity has no apparent influence upon the form of the DSC curves registered. Under such circumstances the rate of heat flow from the sample and container will be determined principally by the thermal characteristics of the sample container and these may be assumed to be constant for a suitable metal container over a small range of temperature.

*Changes in base-line position*

In DSC changes in base-line position before and after a reaction are due to changes in the thermal diffusivity of the sample and become more pronounced in proportion to the heating rate [9]. Thus, if it were possible to design a DSC system in which the thermal diffusivity of the sample would not apparently influence the kinetics of heat flow within the sample, container and fluxmeter assemblage, then

the base-line before and after the reaction would be the same straight line. Experience shows that with suitable container design this is very often the case even when freezing 20 mg or so of pure water within a container (the ratio between the thermal diffusivities of ice and water near to 0° is numerically equal to about 8) and scanning at 0.2 deg a minute. When dealing with saturated porous materials in low temperature DSC the phase transitions occurring within the porous material often involve feeble energy exchange per unit time. Furthermore, the change in the average thermal diffusivity of the sample due to, for example, freezing of water in the pores, is often small, as the porous sample is surrounded by bulk ice. Thus, when cooling large samples, even if there is some derivation of the base-line due to the change in thermal diffusivity of ice with temperature, simple extrapolation of the base-line from -60° to higher temperatures so that it lies under the curve resulting from the phase change water → ice within the pores, is in practice, an accurate way to define the base-line position for the curves associated with the porosity of the sample.

Equation (1) may be fitted to a ballistic DSC curve to investigate how sample and sample container design effect the resolution of a given heat-flow DSC system. In the following section we shall assume that a DSC curve may be exactly fitted to with an equation in the form of equation (1) and discuss how various terms in Eq. (1) may be evaluated in practice.

#### *Analytical study of ballistic DSC curves*

In differential microcalorimetry the area underneath the curve,  $S_c$ , is constant for a given energy signal and is, within limits, practically independent of the thermal characteristics of the sample container, at a given temperature. For an experimental ballistic curve to which Eq. (1) may be fitted we have:

$$\int_{t=0}^{\infty} H \cdot dt = S_c/P = K \frac{\beta^* - \beta}{\beta^* \cdot \beta} \quad (2)$$

where  $P$  is the chart paper speed (assumed constant) and  $K$  is the constant defined implicitly in Eq. (1). Eqs (1) and (2) give:

$$H = \frac{S_c}{P} \cdot \left( \frac{\beta}{1 - \beta/\beta^*} \right) [\exp(-\beta t) - \exp(-\beta^* t)] \quad (3)$$

Inspection of Eq. (3) shows that, for a given energy signal and recorder sensitivity (i.e.  $S_c/P$  constant), the maximum amplitude of  $H$  depends mainly upon the numerical value of  $\beta$ , or in other words, for high resolution of the differential temperature signal in a given DSC system it is desirable that the relaxation curve returns to the base-line as quickly as is possible.

The numerical values of  $\beta$  and  $K$  in Eqs (1) and (2) may be very accurately determined from a plot of  $\ln(H)$  against  $t$ —using numerical values of  $t$  such that

$t > t_1$  where  $t_1$  is a time such that  $\exp(-\beta^*t_1) \rightarrow 0$ . With suitable experimental design it is found that  $t_1$  is approximately the same time at which the temperature measuring thermocouple indicates the finish of a reaction, and which, for reactions giving ballistic curves, practically coincides with the maximum amplitude of the recorded DSC curve. Thus, almost all of the return curve may be used to obtain the straight line relationship between  $\ln(H)$  and  $t$  (this is essentially the method used by Vold [9] to quantify DTA data without knowledge of the sample thermal conductivity). The slope of this straight line gives  $-\beta$  and extrapolation of the line to give an intercept on the  $\ln(H)$  axis ( $t = 0$ ) gives the value of  $\ln(K)$ . The area underneath the DSC ballistic curve,  $S_c$ , may be measured using, for example, polar planimetry and we take this value of  $S_c$  as the value of the area underneath the curve we wish to fit using Eq. (1). Hence the numerical value of  $\beta^*$  may be determined from Eq. (2) i.e.:

$$\beta^* = \left( \frac{\beta PK}{PK - \beta S_c} \right) \quad (4)$$

Assuming that Eq. (1) is an exact fit to the recorded DSC curve we may compute the maximum height of the peak,  $H_x$ , and the time,  $t_x$ , at which this occurs. In addition, we may investigate the dependence of  $H_x$  on the numerical values of  $\beta$  and  $\beta^*$ . The times at which  $H$  has its maximum ( $H_x$ ) and minimum amplitudes may be obtained from Eq. (1) and occur when  $\partial H/\partial t = 0$ , i.e. at times,  $t$ , when:

$$\beta \exp(-\beta t) = \beta^* \exp(-\beta^* t) \quad (5)$$

Solutions of Eq. (5) show that  $H$  has its minimum amplitude, ( $H = 0$ ), when  $t = 0$  or  $t = \infty$  (i.e. on the baseline) and that the maximum,  $H_x$ , occurs at a time  $t_x$  after the start of the quasi-instantaneous reaction given by:

$$t_x = \left( \frac{\ln \beta^* - \ln \beta}{\beta^* - \beta} \right) \quad (6)$$

and the numerical value of  $t_x$  would be constant in a DSC system in which the thermal characteristics of the sample apparently do not influence the values of  $\beta$  and  $\beta^*$  for a given sample container. The value of  $H_x$  may be obtained by substituting  $(\beta/\beta^*) \exp(-\beta t_x)$  from Eq. (5) for  $\exp(-\beta^* t)$  in Eq. (3) which gives the relationship between  $H_x$  and  $t_x$ :

$$H_x = (S_c/P) \beta \exp(-\beta t_x) \quad (7)$$

The conditions for maximum and minimum differential signal resolution in such a DSC system may be deduced from Eqs (6) and (7) and correspond to values of  $\beta$  and  $\beta^*$  such that:

$$\frac{\partial H_x}{\partial \beta} = \frac{\partial}{\partial \beta} \left[ \left( \frac{S_c}{P} \right) \beta \cdot \exp - [\beta(\ln \beta - \ln \beta^*)/(\beta - \beta^*)] \right] = 0 \quad (8)$$

*Use of high resolution DSC to study pore size distributions (PSD)  
in water saturated substances*

Experience in subjecting a variety of rigid or swelling porous materials to a number of freezing and thawing cycles often shows that the endotherms corresponding to ice melting in a particular sample are practically identical curves and evolve over the same temperature range. This would not be the case if the porous structure of the material were significantly altered by the forces arising from the volume change associated with the water  $\rightarrow$  ice phase transition, and it is therefore probable that these forces are dissipated by plastic flow of the ice within the pores and/or that a large number of freezing and thawing cycles are necessary to alter the porous structure.

In a high resolution DSC system a quasi-instantaneous energy signal of magnitude  $E$  gives a peak the height,  $H$ , of which is directly proportional to  $E$  if  $E$  is not too large [4]. This is the case in this microcalorimetric application where the DSC curve is considered as being an envelope corresponding to the summation in time of a very large number of very small quasi-instantaneous energy signals a partial sum of which represents the phase transition energy of the water held in pores of a particular size the phase transition occurring in a time interval  $dt$ .

Let  $T_c$  be the temperature at which water changes phase under equilibrium conditions in pores of Kelvin radius  $r$ . The lowering of phase transition temperature is  $T^*$  and  $T^* = |T_0 - T_c|$ , where  $T_0$  is the temperature at which bulk water changes phase (the ice point). The lowering of transition temperature is often represented by the symbol  $\Delta T$ , but this is confusing in DSC work and, anyway, is not appropriate as the lowering of freezing temperature of water due to capillary effects may be as large  $43.5^\circ$  [2]. Let  $Q$  be the total amount of energy represented by the area underneath a DSC curve which has been obtained using a constant heating rate,  $U$ , ( $U = dT^*/dt$ ) then, [12]:

$$dQ/dt = U \cdot dQ/dT^* = W \cdot H \quad (9)$$

where  $W$  is an accurately known constant which depends upon the recorder sensitivity and where  $H$  is the height of the curve above its baseline. The baseline is the record of the temperature difference between the sample and reference sides of the DSC fluxmeter assemblage when no reaction is occurring (i.e. when  $dQ/dt = 0$ ). Thus  $dQ$  is the energy involved when a volume  $dV$  of water within a porous material changes phase with an apparent phase transition energy  $L(r)$  in a temperature interval  $dT^*$ . Also we suppose that it is possible to exactly fit an equation to the entire DSC curve (occurring over a large temperature interval the magnitude of which depends upon the PSD of the sample) in the form:

$$H(t) = F(T^*) = G(r) \quad (10)$$

where the functions  $F(T^*)$  and  $G(r)$  are determined empirically and permit  $H$  to be computed as a function of  $T^*$  or  $r$  when the scanning rate is  $dT^*/dt$ . Equations (9) and (10) give:

$$dQ = L(r) \cdot dV = (W/U) \cdot H \cdot dT^* = (W/U) \cdot G(r) \cdot dT^* \quad (11)$$

Experimental results using water [2, 13] have shown that  $T^*$  is inversely proportional to  $r$ :

$$T^* = N/r \quad \text{i.e.} \quad dT^* = - (N/r^2) dr \quad (12)$$

where  $N$  is a constant. Combination of Eqs (9), (10), (11) and (12) gives:

$$\frac{dV}{dr} = \frac{-\Omega \cdot G(r)}{r^2 \cdot L(r)} = \frac{-M \cdot G(\psi)}{\psi^2 L(\psi)} \quad (13)$$

where the constant  $\Omega = N \cdot W/U$ ,  $M$  is a constant and  $\psi$  is conveniently defined by  $\psi = 10/T^* = 10r/N$ . Eq. (13) gives the distribution of the size of the pores in a wet porous sample expressed as the derivative of the cumulative pore volume with respect to a pore Kelvin radius. Experimental results obtained using a variety of porous samples show that the function  $G(\psi)$  is often a precise simple Gaussian expression [2, 14]. Some empirical functional relationship between  $T^*$ ,  $L(r)$  and  $r$  have been found [2] and thus, with suitable programmed recording equipment Eq. (13) permits PSD, in a given pore size interval, to be obtained and compared automatically. The technique of plotting the height of a high resolution DSC curve against the reciprocal of the lowering of freezing (or melting) point (the authors " $\psi$  plot") is a powerful tool for investigations and comparisons of PSD in water saturated porous materials and, amongst other things, has been applied to the study of water distribution and the energy associated with migration of interlamella water during freezing and thawing of calcium montmorillonite [2, 5].

The function  $L(r)$  in Eq. (13) is here called the apparent phase transition energy of the pore water because it represents the measured average energy per unit volume of all the water contained within pores of Kelvin radius  $r$ , and therefore is necessarily lower than the energy associated with the freezing of bulk water when unfreezable adsorbed water layers exist on, and near to, the surfaces constituting the walls of the pore spaces.

An experimental procedure permitting high resolution temperature and differential temperature measurements is presented below. To illustrate the effects of sample and sample container design, quasi-instantaneous energy signals of very different magnitudes have been generated within sample containers having very different thermal characteristics. Optimization of the experimental procedure allows a mathematical function in the form of Eq. (1) to be precisely fitted to one of the recorded ballistic DSC curves, and this permits extension of the analysis so that curves occurring over large temperature ranges may be analysed in differential elements.

### Instrumentation

An Arion heat flow microcalorimeter (type MCB) is used. This apparatus possesses an exceptionally sensitive measurement unit (50–60  $\mu\text{V}/\text{mW}$  dissipated). The sample and reference containers have similar thermal characteristics and measure-



ments are made under vacuum to avoid convectational heat losses. The sample temperature,  $T$ , is measured using a thermocouple whose reference junction is placed in a dewar containing a mixture of finely divided ice and distilled water. Distilled water is used to prepare the ice for the reference junction bath. The E.M.F. from the thermopile constituting the fluxmeter constitutes the differential temperature signal (the  $\Delta T$  signal). The  $T$  and  $\Delta T$  signals are amplified using  $\times 100$  gain Sefram high input impedance amplifiers and recorded using a Sefram (type BGD Vat) apparatus. The measured noise level for the differential signal is  $\approx 0.05$  microvolts ( $\mu\text{V}$ ). For quantitative work the most sensitive recorder range used here is such that a  $\Delta T$  (or  $T$ ) signal of magnitude  $5 \mu\text{V}$  gives full scale deflection on the chart recorder.

### *Experimental (A)*

#### *Effect of sample size and sample container design on signal resolution*

Figure 1 shows an exotherm obtained from the freezing of a large sample (278 mg) of pure supercooled water in a heavy stainless steel container of  $0.65 \text{ cm}^3$  capacity. The relaxation curve is exponential. The height of the relaxation curve above its baseline,  $H_m$ , (in cm) is related to the time  $t_m$  (in minutes), measured from an origin co-incident with the start of this quasi-instantaneous energy signal, by the expression:  $H_m \approx 61.46 (\exp - 0.321 t_m)$  this exponential return curve fits the DSC curve at  $t_m \approx 4$  minutes. A ballistic curve, the area underneath which is the same as that of the recorded DSC curve, in the form:

$$H_t = 61.46 [\exp(-0.321 t_m) - \exp(-1.00 t_m)] \quad (14)$$

may be fitted to the experimental curve where  $H_t$  (in cm) is a computed value of the curve height above its baseline (using Eq. 14) for all values of  $t_m$  greater than  $t_0$  (where  $t_0 = 0$  and corresponds with the start of the quasi-instantaneous reaction). A plot of Eq. (14) is shown in Fig. 1 by the thickly dashed line which may be fitted to the DSC curve in this reduced size photograph of the recorded data. The correspondence between the form of the recorded signal and that of a computed one (on the basis of a simple ballistic model) is quite good for many applications. However, for the application discussed here, Eq. (14) does not fit the recorded signal accurately enough which implies that the measuring unit in the calorimeter senses this quasi-instantaneous energy signal as being of relatively long duration due to the time necessary to conduct heat within the sample and through the container walls. Under such circumstances, Eq. (14) would not be applicable as it has the form of Eq. (1) which may only be used to describe ballistic DSC curves resulting from energy signals of very short duration relative to the time constant of the apparatus. However, this is not the only explanation as the reference temperature (not shown) is changed by the large energy signal registered in Fig. 1. This is an undesirable situation which reduces the sensitivity of the measuring unit and introduces difficulties for quantitative analyses. The position of the baseline in Fig. 1 represents the quasi steady state

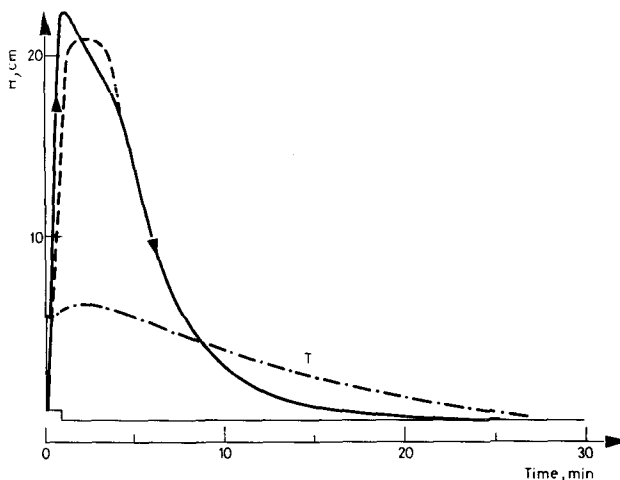


Fig. 1. Exotherm, freezing of 278 mg pure supercooled water in a large container. The ordinate  $H$  is the height of the DSC curve (which has arrows on it) above the base-line as it is drawn in this figure. The heavily dashed line is a plot of Eq. (14). The trace marked "T" (sensitivity 1mv.fsd) is the record of the output of the temperature measuring thermocouple incorporated in the calorimeter. Chart paper speed =  $10 \text{ mm} \cdot \text{min}^{-1}$ ; scanning rate =  $0.2^\circ \text{ min}^{-1}$ ; sensitivity =  $10 \text{ mV. fsd}$

temperature difference between the sample and the reference. The "step" in the baseline, as it is drawn in Fig. 1, is due to an important change in the thermal diffusivity of the sample [9].

The height of the curve above the base-line (shown in Fig. 1) is directly proportional to the temperature difference between the sample and reference sides of the fluxmeter assemblage, relative to an origin which corresponds to the quasi-steady state temperature difference when no reaction is occurring. If the reaction heats the reference side of the fluxmeter, the recorded temperature difference will, of course, be smaller and thus the height of the ballistic curve above the baseline will be proportionally smaller than it would have been if the reaction had not heated the reference. If the DSC curve in Fig. 1 is re-plotted so as to take into consideration the increase in reference temperature due to the reaction (i.e. the ordinate values are appropriately increased so as to be everywhere proportional to the temperature difference between the sample side and reference sides of the fluxmeter when the reference temperature is unaltered by the reaction), then, the DSC curve in Fig. 1 would lie above the curve generated by Eq. (14) and the two curves would have the same form—both showing a "plateau" corresponding to the time necessary to evacuate the heat generated within the sample in its container. Thus, the quickly rising part of the DSC curve in Fig. 1 represents a sudden increase in temperature of the inner surface of the fluxmeter well containing the sample, the energy causing this temperature rise is not sensed as being an instantaneous energy signal due to the thermal characteristics of the large

sample in its poorly conducting sample container and, therefore, the temperature difference (due to the reaction) between the sample and the reference tends to remain constant for some time and this should be represented by a "plateau" on the differential signal (similar in origin to the plateau obtained when an electrical simulation of constant power is maintained for a long time). However, the DSC curve in Fig. 1 has a straight sloping part from the top of the peak to a point where the curve is represented by its relaxation curve (after a time  $\approx 4$  minutes), this is because the energy liberated by the reaction is of such intensity that the reference temperature begins to rise shortly after the maximum of the peak height and thus this straight downward sloping part of the DSC curve does not accurately represent the temperature difference between the sample and the thermostat.

The shape of the DSC curve in Fig. 1 has been discussed in some length as, in an experiment freezing water in a porous material, it could be possible to wrongly interpret such a curve as being due to some supercooling followed by equilibrium freezing of water contained within a porous substance (especially when dealing with porous materials such as some gels where it is often necessary to have an appreciable amount of water in the container so as to have a representative sample). Therefore, for study of these systems special low temperature DSC techniques have to be used [2]. Finally it is noticed that the times necessary for the area underneath the DSC curve in Fig. 1 to have 50, 90 and 98% of its total are 3.3; 8.44 and 13.83 minutes respectively.

Figure 1 shows the sample temperature as recorded by the temperature recording thermocouple (incorporated in the calorimeter as supplied by the manufacturer, and which is located in a cement below and external to the wells at the fluxmeter). For this special application, resolution of temperature measurement is not high enough. This is due to the fact that this thermocouple measures the average temperature of its environment.

For high resolution of the temperature and differential temperature signals the above leads to the conclusion that it would be better to make measurements of the sample temperature nearer to the sample and to have a smaller sample and a smaller sample container of a better conducting metal.

#### *Container design for the study of phase transitions in porous materials*

For accurate measurement of the sample temperature it would be optimum to place a very small, well calibrated thermocouple within the sample; however, for obvious reasons the containers should be vacuum-tight, as well as being large enough to hold a good sized representative sample which is distributed in such a manner that temperature gradients within the sample are minimized. It is also interesting to investigate the effect of cooling rates, so the container must be such that it remains vacuum-tight when quenched. Heat should be conducted to or from the sample uniformly. The amount of heat leaving the sample per unit time is directly proportional to the surface integral in Eq. (15):

$$\frac{\partial Q}{\partial t} = \iint_S Vn \cdot dA \quad (15)$$

where  $Q$  is the amount of heat involved in the reaction and where  $Vn = V \cdot n$  is the component of the velocity  $V$  of heat flow in the direction of the outer normal unit vector  $n$  of the boundary surface,  $S$ , of the sample.

Thus, from Eq. (15) the rate of heat flow from the sample is magnified by increasing the surface area (for a given sample volume) through which heat might flow. Therefore, the sample is held in a special, vacuum-tight highly conducting and thin-walled metal container which in our case has a volume of about  $0.14 \text{ cm}^3$ . A low heat capacity chromel-alumel thermocouple, which is electrically insulated with a thin film of epoxy resin, is placed at the bottom of a cavity existing in a central projection (on the side of the lid in contact with the sample) and has thermal continuity with the very thin layer of metal in intimate contact with the sample, by way of a vacuum grease junction. In conjunction with a slow heating rate, the average temperature of the sample may be known with a precision of about  $\pm 0.02^\circ$ . A perfect thermal contact is assumed to exist between the container and the fluxmeter well, thanks to the thin layer of vacuum grease which joins them. It is difficult to overemphasise the importance of this latter thermal contact and in this connection, it is important to refer to research concerning the thermal conductance, under vacuum of the contact gap between metallic surfaces polished to approximately optical flatness, for various contact pressures [15]. The authors found that the thermal conductance when the surfaces were "just touching" was about the same as when the surfaces were separated by a few millimeters, concluding that heat transfer in this case was by radiation and quoting a radiation conduction of less than  $10^{-3} \text{ watt cm}^{-1} \cdot \text{degree}^{-1}$ .

Various other lid designs [2] incorporating, for example, thermal insulation between the temperature measuring thermocouple well and the metal lid, permit even better temperature resolution. However, with a suitable slow cooling rate, the average temperature of the sample may be known to about  $\pm 0.02^\circ$  when the special all metal small "scanning" containers are used. Figure 2 shows an application and, it is at once evident that even for this still very large (in microcalorimetry) "quasi-instantaneous" energy signal (6.46 J) use of these specially designed small containers facilitates a very accurate fit to the exothermic curve registered. Experience has shown [2, 5] that the relaxation curve in Fig. 2 is independent of sample characteristics for  $0 < |dT/dt| < 2 \text{ deg} \cdot \text{min}^{-1}$  consistent with a situation in which the thermal diffusivity of the sample, apparently, plays no role in determining the way in which the fluxmeter assemblage records an energy signal. Thus, this container design permits accurate analysis of the DSC curve in small temperature increments. Figure 2 shows that an equation, identical in form to Eq. (1), is an exact fit to the ballistic DSC curve registered and this curve is, for practical purposes exactly generated by Eq. (16):

$$H_t = 25.4[\exp(-1.02t_m) - \exp(-6.90t_m)] \quad (16)$$

Thus, in this case 50, 90 and 98% of the total energy signal are registered in 0.844, 2.49 and 4.52 minutes, respectively. The maximum amplitude of the peak ( $H_x = 15.67$  cm) is registered only 19.5 seconds after the start of the quasi-instantaneous energy signal (Eq. (6)) and the height of the return curve above the baseline is equal to half the maximum amplitude of the peak 1.15 minutes after the start of the reaction. Figure 2 also shows that the base-line, before and after the reaction, is the same straight line consistent with "quasi-instantaneous" heat exchange throughout the sample and between the sample and the sample container.

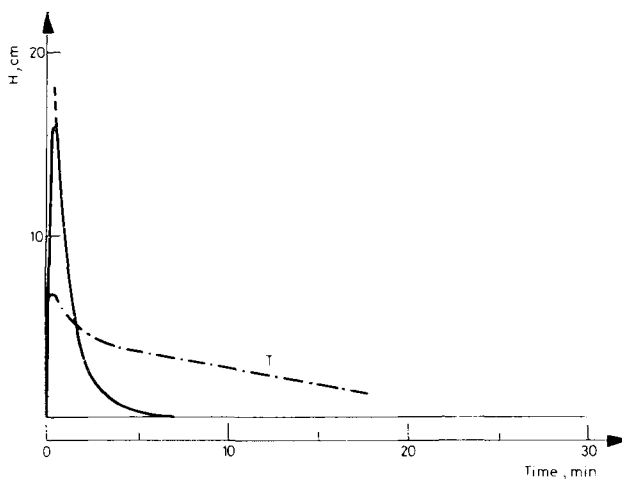


Fig. 2. Exotherm, freezing of 19.4 mg of pure supercooled water in the high resolution system. The trace marked "T" (sensitivity 1mv. fsd) is the output of the temperature measuring thermocouple in intimate contact with the sample. The three dashes represent extrapolation of the exponential relaxation curve. The two superimposable curves are the recorded DSC ballistic curve and a plot of Eq. (16). Chart paper speed = 10 mm. min<sup>-1</sup>; scanning rate = 0.2° min<sup>-1</sup>; sensitivity = 5 mv. fsd

The actual temperature of the sample is much more accurately described when using the special small container, even though the total energy signal is only 7% of that represented in Fig. 1 (both temperature traces were recorded using a full scale recorder sensitivity of 1 mV). The lightly dashed line in Fig. 2 represents extrapolation of the first exponential function in Eq. (16) and the relaxation curve is adequately described by this one exponential function some seconds after the temperature measuring thermocouple records the finish of the reaction. Such a DSC system is very well suited for the study of phase transition within porous materials especially in conjunction with scanning rates of between 0.1 and 0.01 deg min<sup>-1</sup>. Another illustration of the resolution obtainable with such instrumentation is given in Fig. 3 which shows an exotherm obtained from cooling a pure bulk 5.00 M solution of NaCl at the relatively fast rate of 0.5 deg min<sup>-1</sup> in a typical small container. The temperature measuring thermocouple, in

intimate contact with the sample, indicates a temperature difference of  $0.50^\circ$  between the temperatures at which the maxima of the two peaks, are recorded, showing not only that a supercooled eutectic concentration of NaCl is more concentrated than  $5.0 M$  but also that the rate at which the supercooled eutectic is nucleated is much slower than the rate of nucleation of supercooled water (Fig. 2).

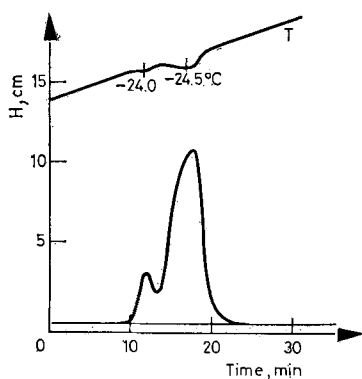


Fig. 3. Exotherm, freezing of pure supercooled  $5.00 M$  NaCl solution in a special scanning container. Chart paper speed =  $5 \text{ mm} \cdot \text{min}^{-1}$ ; scanning rate =  $0.5^\circ \text{ min}^{-1}$ ; sensitivity =  $5 \text{ mv.fsd}$ . The trace marked "T", represents the sample temperature signal (sensitivity  $2.5 \text{ mv.fsd}$ )

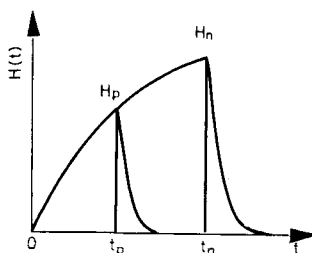


Fig. 4. Evaluation of the portion of the area underneath a high resolution DSC endotherm in the time interval  $t_p \rightarrow t_n$ . See text

With such a high resolution DSC system it is possible to determine very accurately the portion of the area underneath the exotherms or endotherms corresponding to phase changes occurring within porous materials in a known temperature interval. Figure 4) represents part of an endotherm lying between temperatures  $T_p$  and  $T_n$  measured from a time origin coincident with the recorded commencement of the endotherm. Let the height of the curve above its base-line be  $H_n$  at a time  $t_n$ . Because the relaxation curve after a reaction may very accurately be described by a single exponential function some seconds after the temperature measuring thermocouple records the finish of the reaction, we may assume that, were the reaction

to finish at time  $t_n$ , the contribution to the area underneath the curve generated by the return function would be:

$$H_n \int_{t_n}^{\infty} [\exp - \beta(t - t_n)] dt. = \frac{H_n}{\beta} \quad (17)$$

where, for this high resolution system, the proportional heat transfer coefficient,  $\beta$  has the value of  $1.02 \text{ minute}^{-1}$ ; (Eq. (16)).

The portion of the surface area underneath the curve due to ice melting in the porous substance between temperatures  $T_p$  and  $T_n$  is  $\Delta S_{p \rightarrow n}$  and, in practice,

$$\Delta S_{p \rightarrow n} = \int_{t_p}^{t_n} H dt + (H_n - H_p)/\beta \quad (18)$$

With sufficiently slow heating rate the contribution due to the term containing  $\beta$  in Eq. (18) may be made almost negligible small, especially as a DSC curve associated with phase transition in a porous material in which the pore sizes are smaller than about 50 nm Kelvin radius is often a smooth continuous curve where the curve height above its baseline changes slowly with time when  $dT/dt$ , is sufficiently small.

Eqs (17) and (18) are solved using approximate integration techniques where the height of the DSC curve above its baseline is measured directly from the chart paper in unit time increments. This method is particularly suitable for use with inexpensive programmable pocket calculators, and the area underneath the curve is rapidly measured in this way with an accuracy of about  $\pm 0.02\%$ . Numerical integration of data taken directly from the calibrated chart paper obviates problems related to swelling or shrinkage of the chart paper with temperature and humidity. Using this numerical method, data may be abstracted and filed on cards or computer tape. The approach permits an element of the area underneath the exotherm to be compared to the appropriate equivalent portion of area underneath the endotherm. This is useful for investigation of freezing and melting temperature hysteresis in relation to pore form in water saturated porous materials [2, 16].

### *Experimental (B)*

#### *Application to the study of pore size distributions in water saturated porous materials*

The containers are cleaned, dried and polished before being used. The sample is placed inside a container and gently compacted. As the samples are usually water saturated and very fine grained it is assumed that the contact resistances due to a surface "skin" on the inside of the container and a possible air gap between the sample and the container walls are effectively zero.

A vacuum-tight seal is made possible by a silicon-rubber "O" ring. The advantages of this "O" ring are that it may be used from  $-180$  to  $+250^\circ$ , and loses negligible weight when heated at  $160^\circ$  for 48 hours. These "O" rings are kept permanently at

160° before use. Thus, to obtain the "in situ" water content of the sample, the closed container is cleaned externally after the experiment and weighed on a "Mettler" balance ( $\pm 0.1$  mg). The lid is then unscrewed and the wet sample in its container is usually dehydrated by heating at 160° for 15 hours. To avoid water adsorption by the sample during the transit from oven to balance, the lid is carefully screwed back onto the container whilst it is in the oven; the dry sample and container cools to the ambient temperature and the water content is obtained from measuring the weight loss. There is agreement to within about 0.3% with water contents thus measured and with those measured on a separate large aliquot of the sample. The sample container is not directly touched by hand and thus perspiration deposits are avoided. Drying under vacuum at lower temperatures is used in some cases.

*Rapid cooling of a sample.* The thermal geometry of the small container described above permits rapid uniform cooling of the sample, and this is achieved by quickly immersing the sample, in its container, in agitated liquid freon 12 at its fusion temperature ( $-155^\circ$ ). Cooling rates of about  $80 \text{ deg sec}^{-1}$  are often registered. The container is quickly transferred to its place in the fluxmeter well (which is held at a suitable low temperature) tapped one or two times and tested for good thermal contact (by testing the stickiness of the vacuum grease thermal junction between the base of the container and the base of the fluxmeter well) before the system is evacuated for several hours to remove condensation. The assemblage is then heated at a linear, programmed rate to obtain an endotherm corresponding to fusion of ice in a rapidly frozen sample.

## Results

### *Pore size distribution in a water saturated ion-exchange resin*

Experience has shown that in the high resolution DSC system described above, the area underneath the DSC curve for a given energy signal is constant in the temperature interval  $+10^\circ \rightleftharpoons -60^\circ$ .

Figure 5 shows the low temperature exotherm of water freezing in the pore spaces of an Amberlite ion-exchange resin (type XAD-4) which is sold in the form of spherical particles about 1 mm in diameter and is suitable for use in aqueous

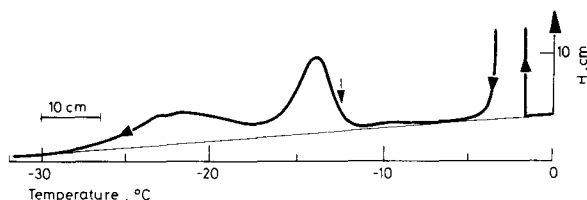


Fig. 5. Exotherm, freezing of a water saturated sample of XAD-4 ion-exchange resin. The ordinate  $H$  is the height of the curve above the base-line as shown in the Figure. At temperatures lower than  $-12.5^\circ\text{C}$  (marked with the vertical arrow) an equation may be precisely fitted to the DSC curve. Sample mass = 0.1709 g dry weight, chart paper speed =  $2.5 \text{ mm} \cdot \text{min}^{-1}$ ; scanning rate =  $0.1^\circ \cdot \text{min}^{-1}$ ; sensitivity =  $0.25 \text{ mv.fsd}$



environments. According to the manufacturers specification [13] this material has a "narrow" pore size distribution with a predominant pore size of 5 nm diameter, a specific surface area of  $750 \text{ m}^2\text{g}^{-1}$  and a porosity of 51%. The vertical arrow at  $-12.5^\circ$  (above the curve in Fig. 5) represents the temperature below which the curve may be adequately fitted to with an equation. The other arrows on the curve in Fig. 5 indicate the sense in which the DSC curve is evolving as a function of the freezing temperature and the scale marked "10 cm" is included on this reduced size photograph of the recorded data to show the dimensions of the experimental curve. (In practice the thickness of the recorded trace is  $\approx 0.05 \text{ mm}$ .)

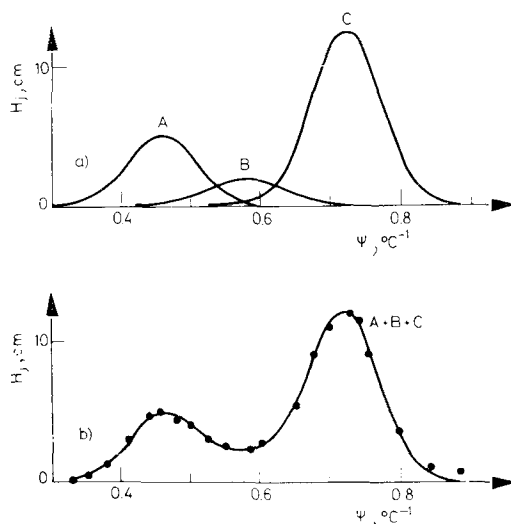


Fig. 6. Interpretation of the data in Fig. 5 using the authors " $\Psi$  plot" ( $\Psi = 10/T_j$ ); 6a: three Gaussian distributions, the sum of which are a precise empirical fit (in the region  $\Psi \leq 0.80$ ) to the recorded DSC curve. Experimental data are shown by the black circles in Figure 6b

Using the authors " $\Psi$  plot" the height of the curve above its baseline  $H_j$  (in cm) at a temperature  $T_j$  (here  $T_j$  is the magnitude of the equilibrium lowering of freezing temperature in  $^\circ$  relative to a zero value at  $0^\circ$ ), is plotted against  $\Psi_j$  ( $\Psi = 10/T_j$ ) and these experimental data are shown by the black circles in Fig. (6b). The continuous curve in Fig. (6b), labelled " $A + B + C$ ", is the summation of three Gaussian distributions A, B and C (shown independently in Fig. 6a) the sum of which constitutes a very good fit to the recorded DSC curve. Each one of the distributions A, B and C is of the form:

$$H_{jk} = \alpha \exp - \gamma(\Psi - \sigma)^2 \quad (19)$$

where  $\alpha$ ,  $\gamma$  and  $\sigma$  are constants for a particular distribution. It is interesting to compare these results with the equation of the DSC endotherm for ice melting in the pore spaces of water saturated calcium montmorillonite [5] and with some results showing that many soils exhibit a moisture characteristic

similar to a normal cumulative distribution function from which the derived pore size distribution is log normal [18].

The computed curve height  $H_{jc} = H_A + H_B + H_C$  is related to the measured trace height  $H_j$  (above the baseline shown in Fig. 5), for the temperature region  $T_j \geq 12.5^\circ$  (i.e.  $\Psi \leq 0.80^{\circ-1}$ ) by the linear regression line:

$$H_j = 1.012 H_{jc} - 0.03, \text{ cm} \quad (20)$$

where the correlation coefficient,  $r_{\text{corr}} = 0.9979$  for all the relevant experimental points shown in Fig. 6b. Integration of  $H_{jc}$  over the temperature interval  $12.5 \leq T_j \leq 30.0^\circ$  in conjunction with the measured (rigorously constant) value of  $dT/dt$  gives a numerical value which agrees with the area underneath the DSC curve correct to 0.03%. The exotherm in Fig. 5 is reproducible after a number of freezing and melting cycles and this could imply that the forces associated with the volume change accompanying the water  $\rightarrow$  ice transition are dissipated by plastic flow of the ice out of the pores rather than changing the porous structure of the resin. Little swelling is observed when the dry resin is saturated with water. It is tentatively concluded, therefore, that the porosity of this wet resin may be represented in terms of three discrete PSD a structure which is not at all evident from analysis of the PSD in the dry resin using nitrogen sorption techniques [2].

The three discrete PSD proposed could refer to the porous regions associated with: the openings of the pores to the external surfaces of the resin beads (these openings control the diffusion of substances into the porosity of the resin); larger pore spaces within the spherical beads of the Amberlite and interconnections between these larger pore spaces [2]. These conclusions are tentative at the moment as there is no independent check upon them, it is hoped to report some more results about the structure of this resin using electron microscopy.

Comparison of the equations fitting the traces of other exotherms and endotherms of water or solutions in porous media is a powerful means of analysing and comparing pore volume and form distributions. Use of a high resolution DSC system permits similar quantification as that shown by Eq. (19), even when analysing freezing or melting behaviour of water in porous materials at temperatures close to  $0^\circ$ . Valuable information concerning the effect of heat on the structure, in the wet state, of synthetic textile fibres with an initial pore diameter when wet of about 65 nm has been obtained using this system [2, 14]. Amongst other things this high resolution technique has been applied to the study of the structure of adsorbed water on a clay surface [2, 19] and to an investigation of the variation with temperature of surface tension at the ice/eutectic interface in porous materials [2].

There appears to be no reason why this technique could not be applied using other microcalorimeters and this would permit calorimetric data related to phase transitions occurring over large temperature intervals to be directly compared and exchanged in the form of equations which fit the curves registered

## References

1. R. DEFAY, I. PRIGOGINE, A. BELLEMANS and D. H. EVERETT, *Surface Tension and Adsorption*, Longmans, Green, London 1966.
2. L. G. HOMSHAW, Ph. D., Thesis, University Paris VII, 1980, 79 p.
3. S. J. GREGG and K. S. W., SING, *Adsorption, Surface Area and Porosity*, p. 139, Academic Press, London 1967.
4. R. CALVET and H. PRAT, *Microcalorimétrie*, Masson et Cie, Paris 1956 (ch. 8).
5. L. G. HOMSHAW, J. CHAUSSIDON, *International Clay Conference, 1978* (ed. M. M. Mortland and V. C. Farmer) 1979, Elsevier Scientific Publishing Company, Amsterdam, p. 141.
6. S. PARTYKA F. ROUQUEROL and J. ROUQUEROL, *J. Colloid Interface Sci.*, 68 (1978) 21.
7. G. LAVILLE, *Compt. Rend. Acad. Sci.*, 240 (1955) 1060.
8. G. LAVILLE, *Compt. Rend. Acad. Sci.*, 240 (1955) 1195.
9. M. J. VOLD, *Anal. Chem.*, 21 (1949) 683.
10. A. D. CUNNINGHAM and F. W. WILBURN, *Differential Thermal Analysis*, (ed. R. C. Mackenzie) Academic Press London, p. 60, 1970.
11. H. S. CARSLAW and J. C. JAEGER, *Conduction of Heat in Solids*, Oxford University Press, Oxford, England 1959.
12. L. G. HOMSHAW, *Compt. Rend. Acad. Sci.* 291 Série B (1980) 31.
13. L. G. HOMSHAW and P. CAMBIER, *J. Soil Sci.*, 31 (1980) 415
14. L. G. HOMSHAW, (to be published)
15. R. B. JACOBS and C. STARR, *Rev. Sci. Instr.*, 10 (1939) 140.
16. L. G. HOMSHAW, *J. Soil. Sci.*, 31 (1980) 399.
17. Serva, *Laboratory products catalogue*, p. 267, Resin XAD-4 pract. Cat. N° 40830, 1978.
18. E. H. D'Hollander, *Water Resources Research.*, 15 (1979).
19. L. G. HOMSHAW and J. P. QUIRK, *Compt. Rend. Acad. Sci.*, 291. Série B (1980) 77.

RÉSUMÉ — La conception appropriée du creuset permet, en analyse calorimétrique différentielle (DSC), une résolution élevée de la température et du signal différentiel, même si des échantillons relativement grands ( $\approx 0.14 \text{ cm}^3$ ) sont utilisés; ainsi des signaux d'énergie associés à des changements de phase ayant lieu dans de larges intervalles de températures peuvent être analysés.

On présente une technique DSC, à haute résolution, originale et efficace, et pour basses températures (la «fonction  $\Psi$ » de l'auteur) pour étudier et comparer les distributions des grandeurs des pores (PSD) dans les échantillons saturés d'eau dont les pores ont des rayons Kelvin entre 1.2 et environ 500 nm, ainsi qu'une application montrant que le PSD dans un échangeur d'ions organiques saturé d'eau peut être obtenu par l'analyse de trois distributions gaussiennes qui fournissent précisément une courbe s'ajustant de façon empirique et excellente au pic exothermique enregistré à basse température et obtenu par congélation de l'eau pure dans l'échantillon.

ZUSAMMENFASSUNG — Die geeignete Behälterformen gestattet sehr hohe Auflösungen der Temperatur und der differentialen Temperatur bei der DSC, auch wenn verhältnismässig grosse ( $\approx 0.14 \text{ cm}^3$ ) Proben verwendet werden; und so können mit über einen weiten Temperaturbereich erfolgenden Phasenänderungen verbundene Energiesignale in unterschiedlichen Elementen analysiert werden.

Eine originale und wirksame DSC-Technik hoher Auflösung bei niedriger Temperatur (die "Funktion  $\Psi$ " des Autors) wird zur Untersuchung und Vergleich von Porengrösseverteilungen (PSD) wassergesättigter Proben für Poren von Kelvin-Radii zwischen 1.2 und etwa 500 nm) gegeben, zusammen mit einer Anwendung, welche zeigt, dass die PSD in einem wassergesättigten organischen Ionenaustauscher aus der Analyse dreier Gauss-schen Verteilungen erhalten werden konnte, die genau eine Kurve ergeben, welche sich dem aufgezeichneten

Niedertemperatur-Exotherm empirisch ausgezeichnet anpasst, das durch Gefrieren von reinem Wasser in der Probe erhalten wurde.

Резюме — С помощью соответствующего приемника были проведены высоко температурные и дифференциально температурные измерения в ДСК даже при использовании относительно больших ( $\approx 0.14 \text{ см}^3$ ) образцов. Энергетические сигналы, связанные с фазовым изменением и протекающие в больших температурных интервалах, могут быть анализированы по различным составным частям. Представлен оригинальный и мощный низкотемпературный метод ДСК высокого разрешения (согласно авторов  $\Psi$  график) для изучения и сравнения распределения размеров проб (РРП) в водонасыщенных образцах для пор, имеющих размеры радиусов Кельвина между 1.2 и 500 нм. Наряду с этим представлено применение этого метода, которое показывает, что РРП в водонасыщенном органическом ионообменнике может быть получено из анализа трех гауссовских распределений, которые точно воспроизводят кривую, которая эмпирически подчиняется регистрируемой низкотемпературной экзотерме, полученной при замораживании чистой воды самом образце.